ChemComm
Chemical Communications

Accepted Manuscript

This article can be cited before page numbers have been issued, to do this please use: I. Squire, M. Tritto, J. Morell and C. Bakewell, *Chem. Commun.*, 2024, DOI: 10.1039/D4CC03904A.

ROYAL SOCIETY OF CHEMISTRY

rsc.li/chemcomm

ChemComm

View Article Online
DOI: 10.1039/D4CC03904A

COMMUNICATION

Probing the reactivity of a transient Al(I) species with substituted arenes

Received 00th January 20xx,
Accepted 00th January 20xx

DOI: 10.1039/x0xx00000x

Imogen Squire,[a] Michelangelo Tritto,[a] Juliana Morell[a] and Clare Bakewell [a]*

With only a handful of compounds known, opportunities to explore the structure and reactivity of dialumenes and related dialumene adducts have been limited. For the first time, a series of dialumene-arene adducts has been synthesised (1-5), from reaction of Al(I) (A) and an aluminium dihydride (B). Adduct formation has been probed experimentally and through DFT, and their reactivity investigated.

Dialumenes, molecules that feature an Al=Al double bond, are a notoriously challenging class of compound to isolate, owing to difficulties in stabilisation of the low oxidation state centre and the subtle difference in coordination environment that are required to favour an Al(I) dimer over a monomer.[1–3] To date, there have been only three examples of isolated dialumenes, all of which are base stabilised.[3–5] In 2017, Inoue and co-workers reported the first neutral Al=Al compound (**I**), with the Al(I) centres stabilised by *N*-heterocyclic carbenes.[4] The integrity of this bond was borne out by DFT, and through reactivity studies with a series of unsaturated molecules which confirmed it reacts as a double bond, forming [2+2] cycloaddition products. This was followed by work from Cowley and Krämer, whose base stabilised dialumene (**II**) was shown to react with alkynes, both as the dialumene and as the Al(I) monomer formed through dissociation of the double bond.[3] Comparison of these two classes of compound shows a significantly different bonding picture. Single crystal X-ray diffraction (SCXRD) reveals a longer Al–Al bond in **II** versus **I**, as well as an increased *trans*-bent geometry. Electron Localisation Function (ELF) and Quantum Theory of Atoms in Molecules (QTAIM) calculations, as well as analysis of the Wiberg Bond Indices all indicate a much weaker, non-classical Al–Al double bond in **II**, with a slipped π-bond structure. This more closely resembles the structure of theoretical base-free RAl=AlR dialumenes.[1]

Prior to the isolation of **I** and **II**, the formation of transient dialumenes had been invoked in the formation of dialumene-arene adducts (**III**, **IV**).[6,7] Tokitoh further showed that **IV** was able to react as a masked source of the dialumene, forming addition products with alkynes and dihydrogen amongst others (Scheme 1b).[8] More recent examples of transient dialumenes and dialumene-arene adducts have also been reported.[9–15]

In 2022 we reported the synthesis of the deuterated dialumene benzene adduct, **1-D**, which was formed through reaction between Roesky's Al(I) complex (**A**) and an amidinate aluminium dihydride (**B**), in benzene solution at elevated temperature (Scheme 1c).[16] The reaction proceeds *via* a series of equilibria involving comproportionation and disproportionation reactions (Scheme 1c, Fig. S1). The product, **1-D**, is proposed to form directly from a transient Al(I) species (monomer (**Al'**) or dimer (**Al.Al**)) and is almost certainly a thermodynamic sink in the complex equilibrium network. According to theoretical calculations on model dialumenes conducted by Cowley and Krämer, electronegative substituents, such as *N*, should lead to a weaker Al–Al bond that more readily dissociates to the Al monomer.[3] The strained 4-membered coordination geometry of the amidinate ligand should also favour weaker Al–Al bonds. This suggests that Al(I) amidinate complexes should be highly reactive species, capable of reacting as either the Al monomer or as the dialumene. However, despite the precedent for **IV** acting as a masked source of Al(I), **1** showed no reaction with a selection of arenes, alkynes or H_2.[16]

This led us to consider the mechanism by which the dialuminum-benzene adduct is formed and if the use of more sterically encumbered or electronically divergent arenes might enable us to

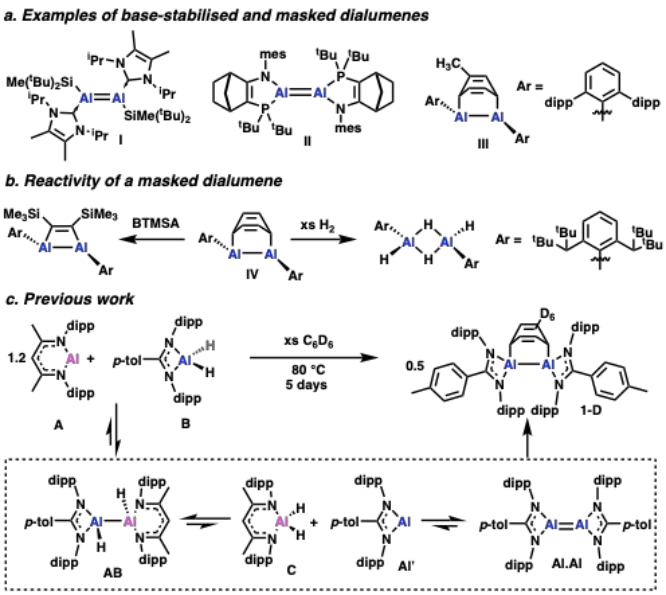

Scheme 1: Examples of isolated and masked dialumenes.

[a] *Dept. of Chemistry, King's College London, 7 Trinity Street, London, SE1 1DB*
Electronic Supplementary Information (ESI) available: [details of any supplementary information available should be included here]. See DOI: 10.1039/x0xx00000x

View Article Online DOI: 10.1039/D4CC03910A

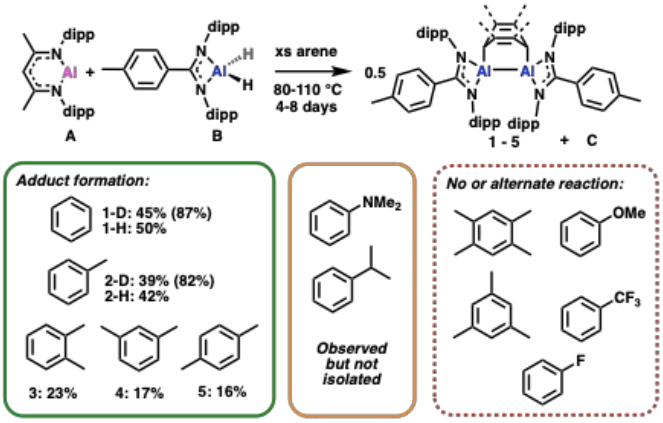

Scheme 2: The formation of dialumene-arene adducts from the reaction of **A** and **B** using a range of substrates. Isolated yields (NMR yields).

access masked reactivity. Herein, we report the reaction of **A** and **B** in the presence of a range of arenes with varying steric and electronic profiles, the resultant dialumene adduct reactivity, as well as computational mechanistic insight.

Heating a mixture comprised of a slight excess of **A**, with **B** in toluene-d_8 at 110 °C (Scheme 2) led to the formation of a bright red solution after 1 hour, with the colour intensifying over 4 days, in line with observations using benzene solvent (**1**). However, analysis of the ^{1}H NMR spectrum revealed a complex mix of products (including **C**, which forms concomitantly with the adduct), with a less distinctive pattern of upfield CH(CH_3)$_2$ doublet environments than was observed in **1** (~0.5 ppm, Fig. S2). Due to the promising colour change, the reaction was continued to work-up, and dark red crystals were isolated (42%).§ SCXRD confirmed formation of a dialumene-toluene adduct (**2-D**), which is directly comparable with **1** (Fig. 1). The Al–Al bond length (2.5520(6) Å) is slightly longer than in **1** (2.5419(7) Å),[16] and similar to that reported for a related toluene adduct.[13] The six-membered ring (C1-C6) bridging the Al atoms shows a pattern of two shorter bonds (C2-C3 1.321(2) Å and C5-C6 1.322(3) Å) opposite each other, and four longer bonds (in the range 1.499(3)-1.510(3) Å), consistent with loss of aromaticity.

Analysis of the ^{1}H NMR spectra showed a complicated set of signals, however formation of the protio-toluene adduct (**2-H**) allowed us to obtain more information. The diene protons, that result from the [2+4] addition of toluene across the dialumene bond (5-6 ppm) indicate two distinct, persistent sets of signals in a ratio that remained consistent between samples (1:0.4, Fig. S3). Exchange spectroscopy (EXSY) spectra show exchange peaks for the *CH$_3$* of the toluene fragment (Fig. S4), as well as for CH and CH_3 environments from the dipp groups (full spectrum Fig. S5), suggesting that the complex exists in two distinct, but slowly interconverting conformations. The two sets of signals are not a result of two different non-interconverting products. Variable temperature (VT) NMR spectroscopy (Figs. S6-8) was used to further probe this. Coalescence was seen for the protons of the toluene fragment when the temperature was increased (T > 55 °C for Al-C*H* and > 95 °C for C=C*H*, Fig. S8), confirming that at room temperature the system is in slow exchange.

With the toluene adduct in hand, we next targeted a series of substituted arenes with varying steric and electronic properties. Firstly, *ortho*-, *para*- and *meta*-xylene were combined with a slight excess of **A** and **B** and heated between 80-100 °C for 5-8 days, with the xylene acting as both substrate and reaction solvent (Scheme 2). Compounds **3-5** were isolated by fractional crystallisation (slow evaporation from hexane). In all cases, crystals suitable for SCXRD were grown, confirming the formation of the respective dialumene-xylene adducts (Fig. 1). The CH_3 groups of the *o*-xylene adduct (**3**) reside on one of the C=C bonds in a 1,2-fashion, in the *m*-xylene adduct (**4**) one CH_3 group is bound to each C=C bond, straddling the Al–C carbon. In both cases, the CH_3 groups reside preferentially on the alkene carbons instead of the Al–C carbons, which is presumably due to a steric preference. Another notable feature of **3** and **5** is that the electron density of the xylene CH_3 groups is localised to one position, indicating no conformational disorder in the crystal. In both **2** and **4** there is conformational disorder leading to CH_3 groups being located at different positions around the diene fragment. However, it is notable that in neither case is there any residual electron density arising from a CH_3 group at the Al-C carbon of the diene fragment.

Unlike with **2**, analysis of the ^{1}H NMR spectra of **3-5** reveals the presence of just one conformational isomer. In each case there are one or two signals corresponding to the Al–C*H* protons in the aliphatic region (**3**, 2.58 (1H, d), 2.75 (1H, d); **4**, 2.44 (1H, s), 2.71 (1H, t); **5**, 2.57 (2H, d) ppm) and the alkene C*H* protons between 5.2-6.4 ppm (**3**, 5.44 (1H, t), 6.33 (1H, determined from COSY as coincident with another resonance, so splitting unobservable); **4**, 5.27 (1H, d), 6.03 (1H, d); **5**, 5.91 (2H, d) ppm) (Figs. S9-10). The presence of two sets of alkene C*H* signals in **3** and **4** suggests a lack of symmetry in the ligand framework, rendering the C*H*s inequivalent; this is also observed in the solid state. Conversely, **5** has a centre of symmetry diagonally through the Al–Al core, leading to equivalent xylene C*H* signals, and in the SCXRD structure there is also a centre of symmetry leading to half the molecule in the asymmetric unit.

The trend towards reduced dialumene-adduct yield with increased steric bulk (16-23% isolated yield **3-5**, *vs*. 39-50% **1-2**), is in line with a less thermodynamically favoured product, which could point to an increased persistence of 'unmasked' Al(I) species in solution. To probe this further, more sterically demanding arenes were investigated. Increasing the number of CH_3 substituents on the arene (mesitylene and durene) did not lead to adduct formation, as

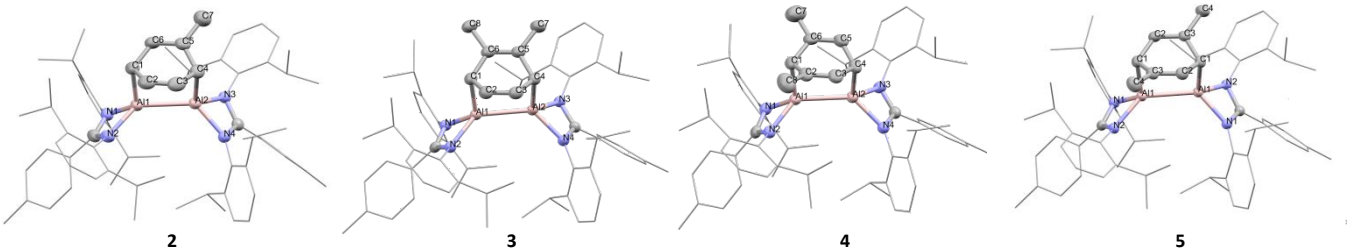

2 **3** **4** **5**

Figure 1: Solid state structures of **2**-**5**. Selected bond lengths (averaged) (Å): **2** Al-Al 2.5520(6), Al1-N1 1.949(1), Al1-C1 2.016(2), C2-C3 1.321(2); **3** Al-Al 2.5485(7), Al1-N1 1.959(1), Al1-C1 2.017(1), C2-C3 1.343(3); **4** Al-Al 2.561(1), Al1-N1 1.973(2), Al1-C1 2.019(2), C2-C3 1.337(2); **5** Al-Al 2.5592(7), Al1-N1 1.953(1), Al1-C1 2.016(2), C2-C3 1.343(2) (full data Tables S1-4).

evidenced by the lack of a distinctive colour change indicative of the dialumene-arene adducts, and an absence of any characteristic signals in the ^{1}H NMR spectra (Fig. S11). However, increasing the steric bulk at the 1-position of the arene did not appear to preclude adduct formation, with both cumene and *N,N*-dimethylaniline forming the characteristic red colour associated with these reactions (Fig. S12). The crude reaction mixtures contain peaks in the alkene region (5-6 ppm) of the ^{1}H NMR spectrum, with cumene showing similar splitting to that seen in the toluene adduct (Fig. S13). However in both cases, repeated attempts to isolate the adduct were unsuccessful.

Due to the highly reactive nature of the equilibrium-based reaction mixture, and the wide range of arene C–E bonds that **A** is known to activate, the scope for testing electron donating and electron withdrawing substituents was limited. For example, despite **A** and **B** immediately forming the asymmetric dihydrodialane intermediate when combined in solution (Fig. S1),[16] reaction of **A** and **B** in anisole at 80 °C led to the known C–O oxidative addition product from reaction of **A** and anisole (Figs. S14-15), along with complex **C** and a previously reported dihydrodialane complex (**D** in Fig. S15).[17–19] The breaking of this C–O bond likely represents a more thermodynamically favoured product, and clearly confirms that the equilibrium reaction that features disproportion and comproportionation reactions between $Al^{I}/Al^{II}/Al^{III}$ intermediates is active in both directions (Fig. S1).

Introduction of electron withdrawing substituents was also limited, as even the C–F bonds in 1-fluorobenzene and α,α,α-trifluorotoluene are known to undergo reaction with **A** under forcing conditions, albeit in an undefined manner. In line with these observations, when **A** and **B** were combined in the presence of trifluorotoluene or fluorobenzene and subjected to the standard reaction conditions a complex mix of products was observed, but with no evidence of the adduct (Figs. S16-18). The presence of several compounds could be identified in the reaction (**C**, ^{dipp}BDIAlF$_2$, ^{dipp}BDIAlHF), which suggests C–F bond activation precludes adduct formation, likely assisted by favourable Al–F bond formation.[20,21]

We next turned to DFT; investigating the [4+1] reaction between **Al'** and benzene, as well the [4+2] reaction from the dialumene (**Al.Al**). Using the full ligand system we tested a range of functionals and basis sets, with M06L/6-31G** (C, H, N) + SDDALL (Al) fou777nd to best support our experimental data (Table S5). Formation of the asymmetric dihydrodialane, **AB**, from **A** and **B** is exergonic, occurring immediately upon mixing and is thus taken as our zero point energy. **AB** disproportionates to **Al'** and **C** (+17.5 kcal mol^{-1}), and dimerisation of **Al'** to **Al.Al** is thermodynamically favoured (-12.3 kcal mol^{-1}), indicating the Al(I) species is more likely to exist as a dialumene. Analysis of the dialumene intermediate (**Al.Al**) reveals a bond length of 2.674 Å, significantly longer than reported for Cowley and Kramer's isolated dialumene (Al–Al 2.5190(14) Å).[3] The Wiberg bond index of 1.12 is also smaller, whilst QTAIM shows a bond critical point (bcp) between the two Al atoms (ρ_{bcp} = 0.05 e/Å^3, $\nabla^2\rho_{bcp}$ = +1.180 e/Å^5, Fig. S26). Taken together, these initial calculations suggest **Al.Al** would have a weaker Al–Al bond and more extreme slipped π-bond character, in line with predictions for an *NN*-ligated species.

Approach of benzene, to **Al.Al**, led to the encounter complex, **Int-1^{di}**, which is slightly endergonic and a transition state for the [4+2] cycloaddition reaction (**TS-1^{di}**) was located, with an energy of 17.1 kcal mol^{-1}, relative to the dialumene (22.3 kcal mol^{-1} relative to **AB**). Here, the ligands are pinched back to allow the approach of the substrate, and the transition state is highly asymmetric, with the ligand at the first Al centre nearly perpendicular with the ligand of the second (Fig. 2). This is similar to a related transition state previously reported by Roesky and co-workers.[13] The transition state leads to **1**, which is the thermodynamically favoured product (-4.5 kcal mol^{-1}). The [4+1] reaction pathway was also investigated, given recent precedent for [4+1] addition products.[16,22,23] A transition state (**TS-1^{mono}**) could be located at 42.9 kcal mol^{-1} relative to **AB**, which proceeds to a high energy intermediate (**Int-2^{mono}**). From here it would be possible for a second equivalent of **Al'** to insert, although it has not been possible to locate a transition state for this process. It therefore seems most likely that **1** is formed via a [4+2] cycloaddition from a dialumene intermediate. The [4+2] pathway was also investigated for toluene and mesitylene substrates. The transition state **TS-1^{di} (tol)** was found to be slightly lower than for benzene (ΔΔG 2.7 kcal mol^{-1}), but **TS-1^{di} (mes)** was significantly higher ((ΔΔG 6.9 kcal mol^{-1}). Moreover, the mesitylene product was found to be thermodynamically unfavoured, compared to **AB**. A combination of both kinetic and thermodynamic effects likely explain why the dialumene adduct is not observed experimentally. Indeed ^{1}H NMR

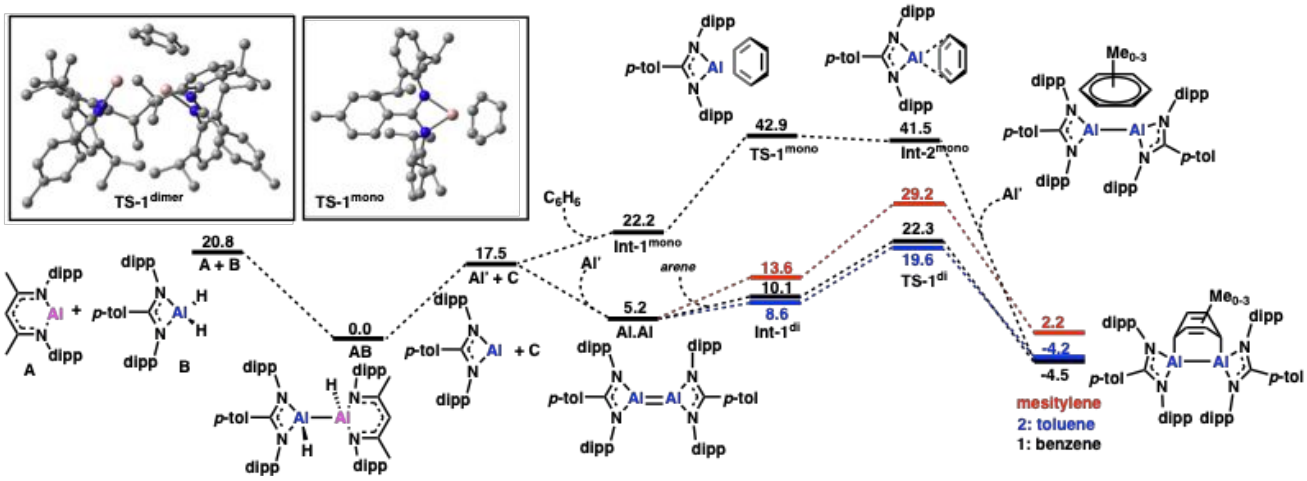

Figure 2: Calculated reaction pathways for the [4+2] and [4+1] cycloaddition reactions between Al(I) species and benzene, toluene and mesitylene. Gibbs free energies (kcal mol^{-1}).

View Article Online
DOI: 10.1039/D4CC03904A

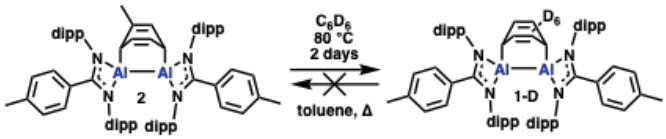

Scheme 3: Reactivity of **1** and **2** with arenes.

investigations show only the presence of **AB** with decomposition occurring over time.

As previously reported, **1** showed no reaction with a range of substrates including H_2 and diphenylacetylene. This is exemplified by the reaction of **1-H** with C_6D_6, where even after prolonged heating the formation of **1-D** was not observed. However, when **2** was heated in benzene-d_6 at 80 °C exchange of the arene ring occurred, and after 2 days full conversion to **1-D** was achieved (Scheme 3; Fig. S18). The reverse reaction of **1** (or **1-D**) in toluene-d_8 showed no change even after prolonged heating at 80 °C, suggesting the **2** is more labile than the equivalent benzene adduct (**1**), and is evidence of a true masked dialumene. This is also supported by DFT, where the transition state for formation of the toluene-dialumene adduct is lower in energy than that of the benzene adduct ($\Delta\Delta G^{\ddagger}$ = 2.7 kcal mol^{-1}).

It could therefore be expected that the transient dialumene formed when **2** is heated may react with other small molecules (Fig. S19). Despite this, no reaction was observed when **2** was exposed to 2 bar of H_2 in cyclohexane-d_{12} or benzene-d_6, although in the latter case arene exchange occurred, forming **1-D** (Fig. S21). This may be a concentration effect, where dialumene formation is too transient to encounter H_2.§§ This points to the proposed dialumene being highly reactive; only stable and persistent enough to react with physically and energetically accessible substrates.

The xylene adducts, **3**-**5,** were shown to be unreactive to both benzene and toluene. This is somewhat surprising, although the transition state to the formation of **3** is slightly higher in energy than for **2** (20.6 kcal mol^{-1}, Fig. S29).

In conclusion, we have synthesised a series of dialumene-arene adducts with varying steric profiles, using a range of substituted arenes. Steric factors were shown to be crucial in determining both if an adduct can be isolated and whether masked reactivity is observed. We can say with certainty that with significant increase in steric hinderance adduct formation becomes less favoured. This is evidenced across the series experimentally and is also born out through DFT. The factors governing the reactivity appear to be subtle and nuanced, not directly attributable to steric factors alone. For example, the toluene-dialumene adduct (**2**) shows evidence of masked reactivity, whereas benzene and xylene derivatives (**1**, **3**-**5**) do not. Nevertheless, this represents the first time that structure activity relationships have been probed for 'masked' dialumenes, and will no doubt inform future attempts to isolate elusive 'free' dialumenes.

CB acknowledges the EPSRC (EP/Y000129/1), Royal Society (RGS R2 222051) and KCL for funding this research. IS acknowledges the NMES faculty (KCL) for studentship funding. We are grateful for the support of Dr Thomas Hicks with NMR experimentation.

Data availability

All data supporting this article have been included as part of the ESI. SCXRD data is available from https://www.ccdc.cam.ac.uk/products/csd/ with deposition numbers 2365635-2365638.

Conflicts of interest

There are no conflicts to declare.

Notes and references

§ Co-crystallisation limited the isolated yield of products **1-2** (~40-45%). However ^{1}H NMR experiments conducted using internal standards showed the % product formed in the reaction to be >80%.
§§ All reactions require an extremely large excess of substrate to form product, with attempts to conduct reactions under more dilute condition unsuccessful. This suggests that the adduct formation is dependent on a high concentration of arene.

1 J. Moilanen, P. P. Power and H. M. Tuononen, *Inorg. Chem.*, 2010, **49**, 10992–11000.
2 K. Hobson, C. J. Carmalt and C. Bakewell, *Chem. Sci.*, 2020, **11**, 6942–6956.
3 R. L. Falconer, K. M. Byrne, G. S. Nichol, T. Krämer and M. J. Cowley, *Angew. Chem. Int. Ed.*, 2021, **60**, 24702–24708.
4 P. Bag, A. Porzelt, P. J. Altmann and S. Inoue, *J. Am. Chem. Soc.*, 2017, **139**, 14384–14387.
5 C. Weetman, A. Porzelt, P. Bag, F. Hanusch and S. Inoue, *Chem. Sci.*, 2020, **11**, 4817–4827.
6 R. J. Wright, A. D. Phillips and P. P. Power, *J. Am. Chem. Soc.*, 2003, **125**, 10784–10785.
7 T. Agou, K. Nagata and N. Tokitoh, *Angew. Chem. Int. Ed.*, 2013, **52**, 10818–10821.
8 K. Nagata, T. Murosaki, T. Agou, T. Sasamori, T. Matsuo and N. Tokitoh, *Angew. Chem. Int. Ed.*, 2016, **55**, 12877–12880.
9 D. Dhara, A. Jayaraman, M. Härterich, R. D. Dewhurst and H. Braunschweig, *Chem. Sci.*, 2022, **13**, 5631–5638.
10 D. Dhara, F. Fantuzzi, M. Härterich, R. D. Dewhurst, I. Krummenacher, M. Arrowsmith, C. Pranckevicius and H. Braunschweig, *Chem. Sci.*, 2022, **13**, 9693–9700.
11 J. D. Queen and P. P. Power, *Chem. Commun.*, 2022, **59**, 43–46.
12 D. Dhara, A. Jayaraman, M. Härterich, M. Arrowsmith, M. Jürgensen, M. Michel and H. Braunschweig, *Chem. Eur. J.*, 2023, **29**, e202300483.
13 A. Kumar, K. Yadav, N. Graw, M. K. Pandey, R. Herbst-Irmer, U. Lourderaj, D. Stalke and H. W. Roesky, *Chem. Eur. J.*, 2023, **29**, e202300546.
14 H. Zhu, S. Fujimori, A. Kostenko and S. Inoue, *Chem. Eur. J.*, 2023, **29**, e202301973.
15 X. Wang, R. F. Ligorio, F. Rüttger, D. Krengel, N. Graw, R. Herbst-Irmer, A. Krawczuk and D. Stalke, *Dalton Trans.*, DOI:10.1039/D4DT01798F.
16 C. Bakewell, K. Hobson and C. J. Carmalt, *Angew. Chem. Int. Ed.*, 2022, **61**, e202205901.
17 R. K. Brown, T. N. Hooper, F. Rekhroukh, A. J. P. White, P. J. Costa and M. R. Crimmin, *Chem. Commun.*, 2021, **57**, 11673–11676.
18 T. Chu, I. Korobkov and G. I. Nikonov, *J. Am. Chem. Soc.*, 2014, **136**, 9195–9202.
19 S. J. Bonyhady, D. Collis, G. Frenking, N. Holzmann, C. Jones and A. Stasch, *Nat. Chem.*, 2010, **2**, 865–869.
20 S. Yow, S. J. Gates, A. J. P. White and M. R. Crimmin, *Angew. Chem. Int. Ed.*, 2012, **51**, 12559–12563.
21 C. Bakewell, A. J. P. White and M. R. Crimmin, *Angew. Chem. Int. Ed.*, 2018, **57**, 6638–6642.
22 D. Sarkar, P. Vasko, A. F. Roper, A. E. Crumpton, M. M. D. Roy, L. P. Griffin, C. Bogle and S. Aldridge, *J. Am. Chem. Soc.*, 2024, **146**, 11792–11800.
23 X. Zhang and L. L. Liu, *Angew. Chem. Int. Ed.*, 2022, **61**, e202116658.

View Article Online
DOI: 10.1039/D4CC03904A

Data availability statement

All data to support the manuscript is included in the supplementary information, or uploaded to the relevant data repositories.

- Data for single crystal X-ray diffraction experiments have been uploaded to the CCDC with data available from https://www.ccdc.cam.ac.uk/ products/csd/ and deposition numbers 2365636 (**2**), 2365635 (**3**), 2365638 (**4**) and 2365637 (**5**). This information is included in the manuscript.
- The DFT coordinates for the calculations discussed in the manuscript are included as supplementary information in the form of a xyz text file.
- All other data is included in the SI document, including NMR spectra of all compounds isolated.